International Journal of Innovative
Computing, Information and Control
Volume **9**, Number **1**, January **2013**

ICIC International ©2013 ISSN 1349-4198
pp. **123–138**

A DICKSON-TYPE ADDER/SUBTRACTOR DC-DC CONVERTER REALIZING STEP-UP/STEP-DOWN CONVERSION

Kei Eguchi[1], Prasit Julsereewong[2], Amphawan Julsereewong[2]
Kuniaki Fujimoto[3] and Hirofumi Sasaki[3]

[1]Department of Information Electronics
Fukuoka Institute of Technology
3-30-1 Wajiro-Higashi, Higashi-Ku, Fukuoka 811-0295, Japan
eguti@fit.ac.jp

[2]Faculty of Engineering
King Mongkut's Institute of Technology Ladkrabang
Ladkrabang, Bangkok 10520, Thailand
{ kjprasit; kcamphaw }@kmitl.ac.th

[3]School of Industrial Engineering
Tokai University
9-1-1 Toroku, Kumamoto-shi, Kumamoto 862-8652, Japan
{ kfuji; hsasaki }@ktmail.tokai-u.jp

Received October 2011; revised February 2012

Abstract. *In this paper, a Dickson-type adder/subtractor DC-DC converter realizing step-up/step-down conversion is proposed. Although the conventional Dickson converter cannot achieve step-up/step-down conversion, the proposed converter can provide not only the stepped-up voltage but also the stepped-down voltage by combining the battery energy and the clean energy. Moreover, the proposed converter can achieve many conversion ratios by utilizing hybrid inputs. Therefore, by choosing the optimal combination of conversion ratio, the proposed converter can alleviate the energy loss caused by the output regulation. To evaluate circuit properties, theoretical analyses, simulations and experiments were performed concerning a simple example of the proposed converter. Circuit simulations and experiments showed the following results: (1) The circuit design is appropriate, because the step-up/step-down conversion was confirmed by the experimental circuit. (2) The number of conversion ratios of the proposed converter is three times as large as that of the conventional three-stage ring-type converter. (3) The proposed converter can reduce more than 25% hardware cost than the conventional converter. (4) The derived theoretical formulas are useful to estimate the characteristics of the proposed converter, because the theoretical result corresponded well with the simulated result.*
Keywords: Charge pump, Step-up/step-down converters, Switching converters, Switched capacitor circuits, Hybrid inputs, Clean energy

1. **Introduction.** A power converter is one of the most important building blocks in electronic products. Among others, a switching DC-DC converter [1-18] is widely used to drive mobile application systems by the stepped-up or the stepped-down voltage, where a lithium-ion battery (Typ. 3.7 V) is usually used as an input source. The switching converter can be divided into two types: an inductor-based converter [1-4] and a capacitor-based converter [5-18].

As a typical inductor-based converter for small power applications, a buck converter, a boost converter and a buck-boost converter are well-known. For example, Dalola et al.

proposed an autonomous sensor system [1] using a boost converter [1-4]. The inductor-based DC-DC converter is efficient at arbitrary conversion ratios. Therefore, the inductor-based converter can realize high power efficiency. However, the inductor-based converter is difficult to be integrated into an IC chip. Moreover, the inductor is often the largest and most expensive component.

On the other hand, the capacitor-based DC-DC converter [5-18] can achieve thin and small circuit composition, light-weight and low-noise, because no magnetic component is necessary. However, the capacitor-based DC-DC converter is efficient only at a few conversion ratios [5-10], because the conversion ratio is predetermined by circuit structure. Therefore, to realize higher power efficiency, the capacitor-based converter which can realize many conversion ratios is desirable. To solve this problem, Chang et al. proposed the multi-stage multiplier/divider DC-DC converter [17, 18], where several switched-capacitor converters are connected mutually to realize many conversion ratios. However, the circuit size extremely increases due to the multi-stage topology though the multi-stage converter can offer various kinds of output voltages.

Recently, being distinct from such approach, the switching converter utilizing clean energy [14-16] has been proposed to save battery energy. For example, Doms et al. proposed capacitive power management circuit [14] using a charge-pump [5-10], where the thermoelectric energy from waste heat [2, 14] is utilized to provide the stepped-up voltage. The capacitor-based converter utilizing clean energy is superior in the point of energy saving. However, like the conventional single-stage converter utilizing battery energy, the capacitor-based converter utilizing clean energy is efficient only at a few conversion ratios, because the circuit topology of the converter utilizing clean energy is the same as that of the single-stage converter utilizing battery energy essentially.

In this paper, a Dickson-type adder/subtractor DC-DC converter is proposed. To generate the output voltage, the proposed converter utilizes two input sources: battery input and clean energy input. Although the conventional Dickson converter [5-10] offers only the $N(= 1, 2, 3, \cdots)\times$ stepped-up voltage, the proposed converter can provide not only the stepped-up voltage but also the stepped-down voltage by combining the battery energy and the clean energy. Moreover, the proposed converter generates various kinds of output voltages compared with the conventional capacitor-based step-up/step-down converter. Therefore, by choosing the optimal combination of conversion ratio, the proposed converter can alleviate the energy loss caused by the output regulation.

To confirm the validity of the circuit design, SPICE simulations and experiments are performed concerning the proposed converter. By comparing the proposed converter with the conventional step-up/step-down converter [11-13], the properties of the proposed converter are evaluated.

2. **Circuit Structure.**

2.1. **Conventional step-up/step-down converter.**

Figure 1 shows an example of the conventional step-up/step-down DC-DC converter [11-13]. The conventional converter of Figure 1 is called the ring-type DC-DC converter. To help readers' understanding, the operation of the ring-type converter is illustrated concerning a simple example shown in Figure 1(b).

The conventional converter of Figure 1(b) consists of twelve power switches and four capacitors. By converting input voltage V_{in}, the conventional converter generates the following output voltage:

$$V_{out} = \frac{s}{r} V_{in}, \tag{1}$$

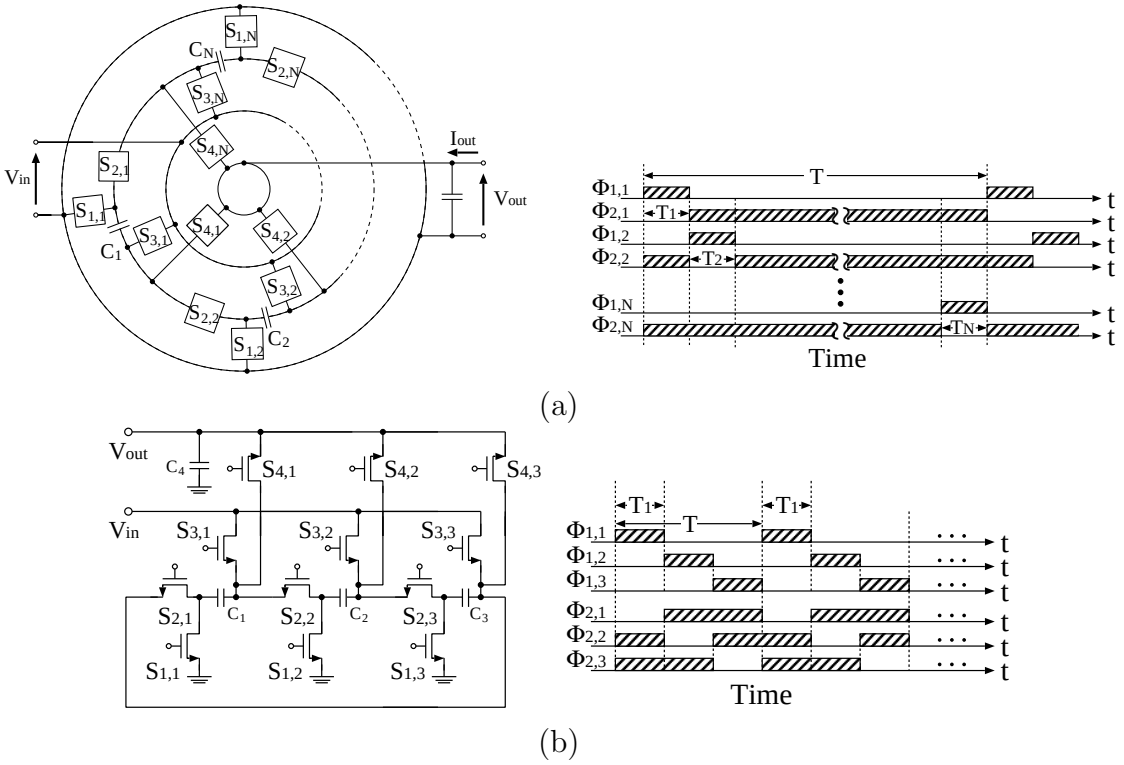

FIGURE 1. Conventional step-up/step-down DC-DC converter [11, 12]: (a) general form and (b) an example of the conventional converter

where parameters s $(= 1, 2, 3)$ and r $(= 1, 2, 3)$ are determined by controlling power switches $S_{i,j}$ $((i = 1, 2, 3)$ and $(j = 1, 2, 3))$. In Figure 1, power switch $S_{1,j}$ is driven by non-overlapped three-phase pulse $\Phi_{1,j}$, $S_{2,j}$ is driven by the inverted pulse of $\Phi_{1,j}$, and $S_{3,j}$ and $S_{4,j}$ are driven by clock pulses obtained by shifting clock pulses $\Phi_{1,j}$ cyclically.

In Figure 1(b), the number of capacitors connected to the input terminal in series through $S_{3,j}$, $S_{2,j}$ and $S_{1,j}$ is fixed to r. On the other hand, the number of capacitors connected to the output terminal in series through $S_{4,j}$, $S_{2,j}$ and $S_{1,j}$ is fixed to s. Consequently, the stepped-up/stepped-down voltage $(s/r)V_{in}$ is obtained as an output voltage. In other words, the conventional converter is the multiplier/divider DC-DC converter [11-13, 17, 18]. In Figure 1(b), the conventional converter can realize seven types of conversion ratio: $s/r = \{1/3, 1/2, 2/3, 1, 2, 3/2, 3\}$. As (1) shows, the number of conversion ratios is determined by the number of capacitors.

2.2. **Proposed converter.** Figure 2 shows the proposed adder/subtractor DC-DC converter utilizing two input sources: battery input and clean energy input. To help readers' understanding, the operation of the proposed converter is illustrated concerning a simple example shown in Figure 2(b).

By combining the battery energy and the clean energy, the proposed converter generates the stepped-up/stepped-down voltage as follows:

$$V_{out} = \{V_1 - (V_{in1} \vee V_{in2} \vee 0)\} + (V_{in1} \vee V_{in2} \vee 0), \tag{2}$$

where $V_1 = \{(V_{in1} \vee V_{in2}) - (V_{in1} \vee V_{in2} \vee 0)\} + (V_{in1} \vee V_{in2} \vee 0)$.

As (1) and (2) show, the conversion method of the proposed converter is totally different from that of the conventional converter. In the proposed adder/subtractor DC-DC converter, the number of conversion ratios is determined by not only the number of capacitors but also the number of inputs. By controlling power switches as shown in Table

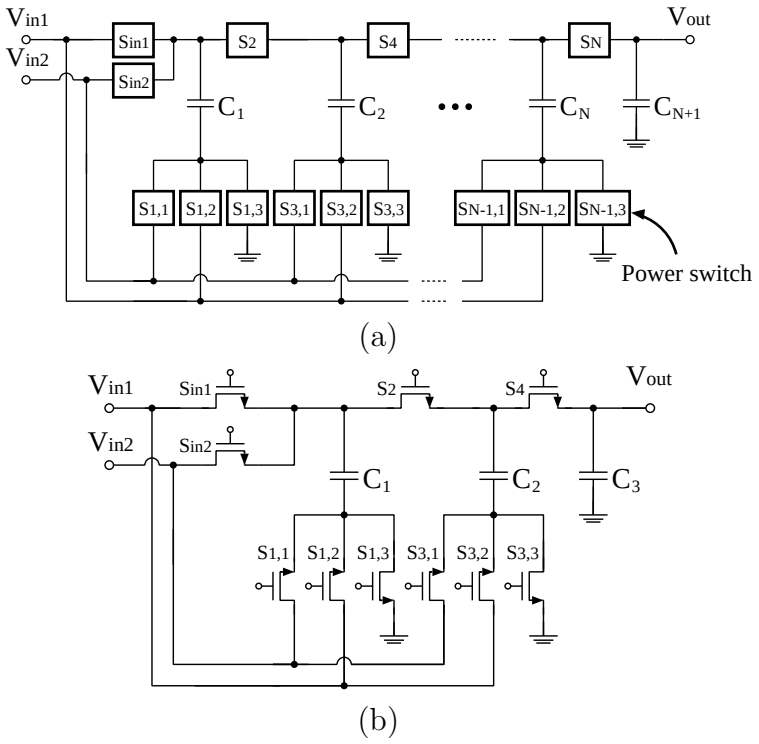

FIGURE 2. Proposed converter: (a) general form and (b) an example of the proposed converter in the case of $N = 3$

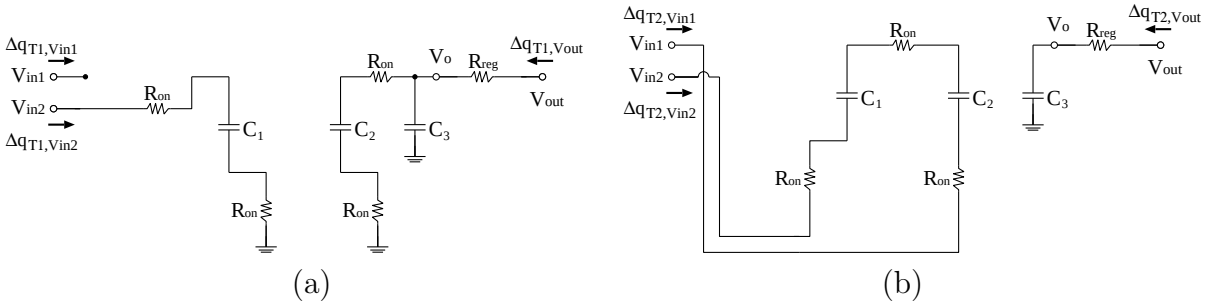

FIGURE 3. Instantaneous equivalent circuits of the proposed converter in the case of No.13: (a) $State - T1$ and (b) $State - T2$

1, the proposed converter can achieve twenty conversion ratios, where $V_{in1} \neq V_{in2}$ and $V_{out} > 0$. Table 2 shows the comparison between the proposed converter of Figure 2(b) and the conventional converter of Figure 1(b). As Table 2 shows, the proposed converter can provide various kinds of output voltages than the conventional converter. Therefore, by choosing the optimal combination of conversion ratio, the proposed converter can alleviate the energy loss caused by the output regulation. Moreover, the proposed converter can realize hardware size smaller than the conventional converter. In the development of mobile application systems, it is clear that a small circuit is advantageous.

The properties of the proposed converter will be analyzed in the following section.

3. **Theoretical Analysis.** In the IC design of capacitor-based converters, the effect of on-resistance on the power efficiency is one of the most important properties, because the most of the chip area are occupied by power switches. Therefore, the properties concerning power efficiency and on-resistance are clarified theoretically. Moreover, in

TABLE 1. Setting of clock pulses

No.	Output V_{out}	State	On	Off
1	V_{in1}	$T1$	S_{in1}, $S_{1,3}$, $S_{3,3}$, S_4	Other switches
		$T2$	$S_{1,3}$, S_2, $S_{3,3}$	Other switches
2	V_{in2}	$T1$	S_{in2}, $S_{1,3}$, $S_{3,3}$, S_4	Other switches
		$T2$	$S_{1,3}$, S_2, $S_{3,3}$	Other switches
3	$2V_{in1}$	$T1$	S_{in1}, $S_{1,3}$, $S_{3,3}$, S_4	Other switches
		$T2$	$S_{1,2}$, S_2, $S_{3,3}$	Other switches
4	$2V_{in2}$	$T1$	S_{in2}, $S_{1,3}$, $S_{3,3}$, S_4	Other switches
		$T2$	$S_{1,1}$, S_2, $S_{3,3}$	Other switches
5	$3V_{in1}$	$T1$	S_{in1}, $S_{1,3}$, $S_{3,2}$, S_4	Other switches
		$T2$	$S_{1,2}$, S_2, $S_{3,3}$	Other switches
6	$3V_{in2}$	$T1$	S_{in2}, $S_{1,3}$, $S_{3,1}$, S_4	Other switches
		$T2$	$S_{1,1}$, S_2, $S_{3,3}$	Other switches
7	$V_{in1} + V_{in2}$	$T1$	S_{in1}, $S_{1,3}$, $S_{3,3}$, S_4	Other switches
		$T2$	$S_{1,1}$, S_2, $S_{3,3}$	Other switches
8	$2V_{in1} + V_{in2}$	$T1$	S_{in1}, $S_{1,3}$, $S_{3,1}$, S_4	Other switches
		$T2$	$S_{1,2}$, S_2, $S_{3,3}$	Other switches
9	$V_{in1} + 2V_{in2}$	$T1$	S_{in1}, $S_{1,3}$, $S_{3,1}$, S_4	Other switches
		$T2$	$S_{1,1}$, S_2, $S_{3,3}$	Other switches
10	$V_{in1} - V_{in2}$	$T1$	S_{in1}, $S_{1,1}$, $S_{3,3}$, S_4	Other switches
		$T2$	$S_{1,3}$, S_2, $S_{3,3}$	Other switches
11	$2V_{in1} - V_{in2}$	$T1$	S_{in1}, $S_{1,3}$, $S_{3,3}$, S_4	Other switches
		$T2$	$S_{1,2}$, S_2, $S_{3,1}$	Other switches
12	$V_{in1} - 2V_{in2}$	$T1$	S_{in1}, $S_{1,1}$, $S_{3,3}$, S_4	Other switches
		$T2$	$S_{1,3}$, S_2, $S_{3,1}$	Other switches
13	$2V_{in2} - V_{in1}$	$T1$	S_{in2}, $S_{1,3}$, $S_{3,3}$, S_4	Other switches
		$T2$	$S_{1,1}$, S_2, $S_{3,2}$	Other switches
14	$V_{in2} - 2V_{in1}$	$T1$	S_{in2}, $S_{1,2}$, $S_{3,3}$, S_4	Other switches
		$T2$	$S_{1,3}$, S_2, $S_{3,2}$	Other switches
15	$2V_{in1} - 2V_{in2}$	$T1$	S_{in1}, $S_{1,1}$, $S_{3,3}$, S_4	Other switches
		$T2$	$S_{1,2}$, S_2, $S_{3,1}$	Other switches
16	$2V_{in2} - 2V_{in1}$	$T1$	S_{in2}, $S_{1,2}$, $S_{3,3}$, S_4	Other switches
		$T2$	$S_{1,1}$, S_2, $S_{3,2}$	Other switches
17	$3V_{in1} - V_{in2}$	$T1$	S_{in1}, $S_{1,1}$, $S_{3,2}$, S_4	Other switches
		$T2$	$S_{1,2}$, S_2, $S_{3,3}$	Other switches
18	$3V_{in1} - 2V_{in2}$	$T1$	S_{in1}, $S_{1,1}$, $S_{3,2}$, S_4	Other switches
		$T2$	$S_{1,2}$, S_2, $S_{3,1}$	Other switches
19	$3V_{in2} - V_{in1}$	$T1$	S_{in2}, $S_{1,2}$, $S_{3,1}$, S_4	Other switches
		$T2$	$S_{1,1}$, S_2, $S_{3,3}$	Other switches
20	$3V_{in2} - 2V_{in1}$	$T1$	S_{in2}, $S_{1,2}$, $S_{3,1}$, S_4	Other switches
		$T2$	$S_{1,1}$, S_2, $S_{3,2}$	Other switches

order to evaluate the characteristics of the proposed converter, the comparison between the proposed converter and the conventional ring-type converter is performed theoretically.

To save space, only the theoretical analysis in the case of No.13 ($V_{out} = 2V_{in2} - V_{in1}$) and No.18 ($V_{out} = 3V_{in1} - 2V_{in2}$) is discussed in this section. The theoretical analysis is performed under the conditions that 1. Since the proposed converter is not operated at

TABLE 2. Comparison concerning hardware cost and conversion ratio

	Number of capacitors	Number of switches	Number of conversion ratios
Proposed converter	3	10	20
Conventional converter	4	14	7

high frequency, the influence of parasitic elements is negligibly small, and 2. To evaluate the maximum power efficiency, the time constant is much larger than the period of clock pulses.

3.1. **Analysis for No.13.** In a steady state, the instantaneous equivalent circuits of the proposed converter can be expressed by the circuits shown in Figure 3, where R_{on} denotes the on-resistance of the power switch. In Figure 3, the differential value of the electric charge in capacitor C_k $(k = 1, 2, 3)$ satisfies

$$\Delta q^k_{T1} + \Delta q^k_{T2} = 0, \quad \text{where } T = T1 + T2, \quad T1 = DT \quad \text{and} \quad T2 = (1 - D)T. \tag{3}$$

In (3), D is the duty factor, and Δq^k_{T1} and Δq^k_{T2} denote electric charges in the case of $State - T1$ and $State - T2$, respectively.

In the case of $State-T1$, differential values of electric charges in terminal V_{in1}, terminal V_{in2} and terminal V_{out}, $\Delta q_{T1,V_{in1}}$, $\Delta q_{T1,V_{in2}}$ and $\Delta q_{T1,V_{out}}$, are given by

$$\Delta q_{T1,V_{in1}} = 0, \quad \Delta q_{T1,V_{in2}} = \Delta q^1_{T1} \quad \text{and} \quad \Delta q_{T1,V_{out}} = \Delta q^2_{T1} + \Delta q^3_{T1}. \tag{4}$$

On the other hand, in the case of $State - T2$, differential values of electric charges in terminal V_{in1}, terminal V_{in2} and terminal V_{out}, $\Delta q_{T2,V_{in1}}$, $\Delta q_{T2,V_{in2}}$ and $\Delta q_{T2,V_{out}}$, are given by

$$\Delta q_{T2,V_{in1}} = -\Delta q^2_{T2}, \quad \Delta q_{T2,V_{in2}} = -\Delta q^1_{T2} \quad \text{and} \quad \Delta q_{T2,V_{out}} = \Delta q^3_{T2}, \tag{5}$$

where $\Delta q^1_{T2} = -\Delta q^2_{T2}$.

Using (4) and (5), average currents in the input terminals and the output terminal can be expressed by

$$\begin{aligned} \overline{I_{in1}} &= (\Delta q_{T1,V_{in1}} + \Delta q_{T2,V_{in1}})/T := \Delta q_{V_{in1}}/T, \\ \overline{I_{in2}} &= (\Delta q_{T1,V_{in2}} + \Delta q_{T2,V_{in2}})/T := \Delta q_{V_{in2}}/T \\ \text{and} \quad \overline{I_{out}} &= (\Delta q_{T1,V_{out}} + \Delta q_{T2,V_{out}})/T := \Delta q_{V_{out}}/T, \end{aligned} \tag{6}$$

where $\Delta q_{V_{in1}}$, $\Delta q_{V_{in2}}$ and $\Delta q_{V_{out}}$ are electric charges in terminal V_{in1}, terminal V_{in2} and terminal V_{out}, respectively.

Therefore, from (3)-(6), we have the relation between average output current $\overline{I_{out}}$ and average input currents $\overline{I_{in1}}$ and $\overline{I_{in2}}$ as follows:

$$\overline{I_{in1}} = \overline{I_{out}} \quad \text{and} \quad \overline{I_{in2}} = -2\overline{I_{out}}. \tag{7}$$

Next, let us consider the consumed energy in one period. In Figure 3, the consumed energy in one period, W_T, can be expressed as

$$W_T = W_{T1} + W_{T2}, \tag{8}$$

where

$$W_{T1} = \frac{2R_{on}}{T1}(\Delta q^1_{T1})^2 + \frac{2R_{on}}{T1}(\Delta q^2_{T1})^2 \quad \text{and} \quad W_{T2} = \frac{3R_{on}}{T2}(\Delta q^1_{T2})^2. \tag{9}$$

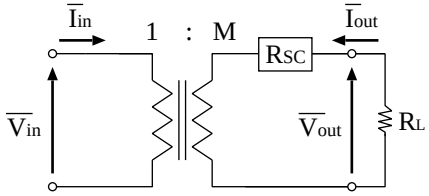

FIGURE 4. General form of the equivalent circuit

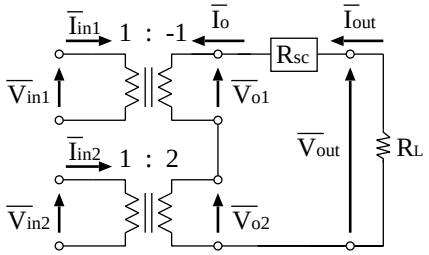

FIGURE 5. Equivalent circuit of the proposed converter in the case of No.13 ($V_{out} = 2V_{in2} - V_{in1}$)

Using (3)-(6), consumed energy (9) can be rewritten as

$$W_T = \frac{(4-D)R_{on}}{D(1-D)T}(\Delta q_{V_{out}})^2. \tag{10}$$

Here, a general equivalent circuit of SC power converters [15,16] can be given by the circuit shown in Figure 4. In Figure 4, R_{SC} is called the SC resistance, M is the ratio of an ideal transformer, and $\overline{V_{in}}$ and $\overline{V_{out}}$ denote the average input voltage and the average output voltage, respectively. The consumed energy W_T in Figure 4 can be expressed as

$$W_T = W_{T1} + W_{T2} := \left(\frac{\Delta q_{V_{out}}}{T}\right)^2 \cdot R_{SC} \cdot T. \tag{11}$$

Therefore, from (10) and (11), SC resistance R_{SC} of the proposed converter is expressed as

$$R_{SC} = \frac{(4-D)}{D(1-D)} \cdot R_{on}. \tag{12}$$

Using (7) and (12), the equivalent circuit in the case of No.13 can be expressed by the following determinant:

$$\begin{bmatrix} \overline{V_{in1}} \\ \overline{I_{in1}} \end{bmatrix} = \begin{bmatrix} -1 & 0 \\ 0 & -1 \end{bmatrix} \begin{bmatrix} \overline{V_{o1}} \\ -\overline{I_o} \end{bmatrix}, \quad \begin{bmatrix} \overline{V_{in2}} \\ \overline{I_{in2}} \end{bmatrix} = \begin{bmatrix} 1/2 & 0 \\ 0 & 2 \end{bmatrix} \begin{bmatrix} \overline{V_{o2}} \\ -\overline{I_o} \end{bmatrix}$$

$$\text{and} \quad \begin{bmatrix} \overline{V_{o1}} + \overline{V_{o2}} \\ \overline{I_o} \end{bmatrix} = \begin{bmatrix} 1 & R_{SC} \\ 0 & 1 \end{bmatrix} \begin{bmatrix} \overline{V_{out}} \\ \overline{I_{out}} \end{bmatrix}, \tag{13}$$

because the equivalent circuit of the SC power converters can be expressed by the determinant using the Kettenmatrix. Finally, from (13), we have the equivalent circuit of the proposed converter as shown in Figure 5. From Figure 5, the power efficiency η_p and the

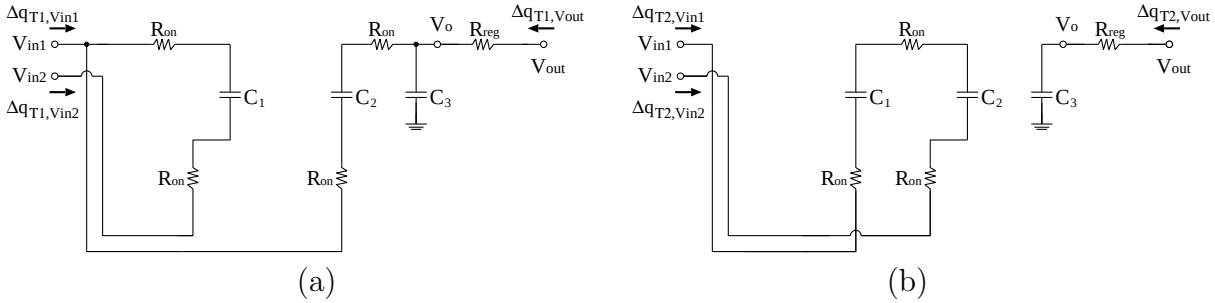

FIGURE 6. Instantaneous equivalent circuits of the proposed converter in the case of No.18: (a) $State - T1$ and (b) $State - T2$

output voltage V_{out} [1] of the proposed converter are obtained as

$$\eta_p = \frac{(\overline{I_{out}})^2 R_L}{(\overline{I_{out}})^2 R_{SC} + (\overline{I_{out}})^2 R_L} = \frac{R_L}{R_{SC} + R_L} \tag{14}$$

$$\text{and} \qquad V_{out} = \frac{R_L}{R_{SC} + R_L}(2V_{in2} - V_{in1}), \tag{15}$$

where R_L denotes the output load.

For example, the target voltage such as 2.2 V is required to drive a center processing unit (CPU). In the case of No.13, the ideal output voltage of the proposed converter is obtained by

$$V_{out} = 2V_{in2} - V_{in1} = 2.3\,\text{V} \tag{16}$$

if the input voltages are $V_{in1} = 3.7\,\text{V}$ and $V_{in2} = 3\,\text{V}$ [2]. As (16) shows, the energy loss due to the output regulation in the proposed converter is smaller than that in the conventional converter, because the conventional converter generates the target voltage by regulating the $2/3 \times$ stepped-down voltage ($\simeq 2.47\,\text{V}$). Concretely, the voltage efficiency V_{tag}/V_{out} of the proposed converter and the conventional converter is 95.7% and 89.2%, respectively. That is, the proposed converter can improve voltage efficiency about 6% from the conventional converter.

3.2. **Analysis for No.18.** Figure 6 shows the instantaneous equivalent circuits of the proposed converter in the case of No.18. In the case of $State - T1$, $\Delta q_{T1,V_{in1}}$, $\Delta q_{T1,V_{in2}}$ and $\Delta q_{T1,V_{out}}$ are given by

$$\Delta q_{T1,V_{in1}} = \Delta q^1_{T1} - \Delta q^2_{T1}, \quad \Delta q_{T1,V_{in2}} = -\Delta q^1_{T1} \quad \text{and} \quad \Delta q_{T1,V_{out}} = \Delta q^2_{T1} + \Delta q^3_{T1}. \tag{17}$$

On the other hand, in the case of $State - T2$, $\Delta q_{T2,V_{in1}}$, $\Delta q_{T2,V_{in2}}$ and $\Delta q_{T2,V_{out}}$ are given by

$$\Delta q_{T2,V_{in1}} = -\Delta q^1_{T2}, \quad \Delta q_{T2,V_{in2}} = -\Delta q^2_{T2} \quad \text{and} \quad \Delta q_{T2,V_{out}} = \Delta q^3_{T2}, \tag{18}$$

where $\Delta q^1_{T2} = -\Delta q^2_{T2}$.

Therefore, from (3), (6), (17) and (18), we have the following relation concerning currents:

$$\overline{I_{in1}} = -3\overline{I_{out}} \quad \text{and} \quad \overline{I_{in2}} = 2\overline{I_{out}}. \tag{19}$$

[1]Of course, the consumed energy of peripheral circuits such as pulse generators and comparators is disregarded in the power efficiency of (14).

[2]The input sources V_{in1} and V_{in2} were assumed as a lithium battery and a thermoelectric generator (TEG).

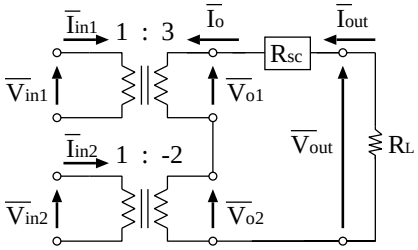

FIGURE 7. Equivalent circuit of the proposed converter in the case of No.18 ($V_{out} = 3V_{in1} - 2V_{in2}$)

In Figure 6, the consumed energy in $State - T1$ and $State - T2$ is expressed as

$$W_{T1} = \frac{2R_{on}}{T1}(\Delta q_{T1}^1)^2 + \frac{2R_{on}}{T1}(\Delta q_{T1}^2)^2 \quad \text{and} \quad W_{T2} = \frac{3R_{on}}{T2}(\Delta q_{T2}^1)^2. \tag{20}$$

Using (11), (17) and (18), (20) can be rewritten as

$$W_T = \frac{(4-D)R_{on}}{D(1-D)T}(\Delta q_{V_{out}})^2. \tag{21}$$

Therefore, from (11) and (21), we have the SC resistance as follows:

$$R_{SC} = \frac{(4-D)}{D(1-D)} \cdot R_{on} \tag{22}$$

Using (19) and (22), the equivalent circuit in the case of No.18 can be expressed by the following determinants:

$$\begin{bmatrix} \overline{V_{in1}} \\ \overline{I_{in1}} \end{bmatrix} = \begin{bmatrix} 1/3 & 0 \\ 0 & 3 \end{bmatrix} \begin{bmatrix} \overline{V_{o1}} \\ -\overline{I_o} \end{bmatrix}, \quad \begin{bmatrix} \overline{V_{in2}} \\ \overline{I_{in2}} \end{bmatrix} = \begin{bmatrix} -1/2 & 0 \\ 0 & -2 \end{bmatrix} \begin{bmatrix} \overline{V_{o2}} \\ -\overline{I_o} \end{bmatrix}$$
$$\text{and} \quad \begin{bmatrix} \overline{V_{o1}} + \overline{V_{o2}} \\ \overline{I_o} \end{bmatrix} = \begin{bmatrix} 1 & R_{SC} \\ 0 & 1 \end{bmatrix} \begin{bmatrix} \overline{V_{out}} \\ \overline{I_{out}} \end{bmatrix}. \tag{23}$$

Finally, from (23), we have the equivalent circuit of the proposed converter as shown in Figure 7. From Figure 7, the power efficiency η_p and the output voltage V_{out} are obtained as

$$\eta_p = \frac{(\overline{I_{out}})^2 R_L}{(\overline{I_{out}})^2 R_{SC} + (\overline{I_{out}})^2 R_L} = \frac{R_L}{R_{SC} + R_L} \tag{24}$$

$$\text{and} \qquad V_{out} = \frac{R_L}{R_{SC} + R_L}(3V_{in1} - 2V_{in2}). \tag{25}$$

For example, the target voltage such as 5 V is required to drive LED (Light Emitting Diode) backlighting. In the case of No.18, the ideal output voltage of the proposed converter is obtained by

$$V_{out} = 3V_{in1} - 2V_{in2} = 5.1\,\text{V} \tag{26}$$

if the input voltages are $V_{in1} = 3.7$ V and $V_{in2} = 3$ V. As (26) shows, the energy loss due to the output regulation in the proposed converter is smaller than that in the conventional converter, because the conventional converter generates the target voltage by regulating the $3/2\times$ stepped-up voltage ($\simeq 5.55$ V). Concretely, the voltage efficiency V_{tag}/V_{out} of the proposed converter and the conventional converter is 90.1% and 98.0%, respectively. That is, the proposed converter can improve voltage efficiency about 8% from the conventional converter.

To save space, only the power efficiency in the case of No.13 and No.18 was discussed in this paper. However, other modes can also be analyzed by the same method.

TABLE 3. Comparison concerning power efficiency in the case of step-down conversion

Proposed	SC resistance	Efficiency	Output voltage
	$R_{SC.p}$	η_p	$V_{out.p}$
($V_{tag} = 2.2\,\mathrm{V}$)	$\dfrac{(4-D)}{D(1-D)} \cdot R_{on}$	$\dfrac{R_L}{R_L + R_{SC.p}}$	$\dfrac{R_L}{R_L + R_{SC.p}}(2V_{in2} - V_{in1})$
Conventional	SC resistance	Efficiency	Output voltage
	$R_{SC.c}$	η_c	$V_{out.c}$
($V_{tag} = 2.2\,\mathrm{V}$)	$\dfrac{19}{9} \cdot R_{on}$	$\dfrac{R_L}{R_L + R_{SC.c}}$	$\dfrac{R_L}{R_L + R_{SC.c}}\left(\dfrac{2V_{in1}}{3}\right)$

TABLE 4. Comparison concerning power efficiency in the case of step-up conversion

Proposed	SC resistance	Efficiency	Output voltage
	$R_{SC.p}$	η_p	$V_{out.p}$
($V_{tag} = 5\,\mathrm{V}$)	$\dfrac{(4-D)}{D(1-D)} \cdot R_{on}$	$\dfrac{R_L}{R_L + R_{SC.p}}$	$\dfrac{R_L}{R_L + R_{SC.p}}(2V_{in2} - V_{in1})$
Conventional	SC resistance	Efficiency	Output voltage
	$R_{SC.c}$	η_c	$V_{out.c}$
($V_{tag} = 5\,\mathrm{V}$)	$\dfrac{19}{4} \cdot R_{on}$	$\dfrac{R_L}{R_L + R_{SC.c}}$	$\dfrac{R_L}{R_L + R_{SC.c}}\left(\dfrac{3V_{in1}}{2}\right)$

3.3. **Comparison.** In this subsection, the comparison concerning power efficiency is discussed. Tables 3 and 4 show the summary of the theoretical results, where the theoretical analysis concerning the conventional ring-type converter will be discussed in Appendix. Since the output voltage is regulated to provide the target output voltage, the total efficiency $\eta_{total.p}$ of the proposed converter is expressed as

$$\eta_{total.p} = \eta_{reg.p} \times \eta_p, \tag{27}$$

where $\eta_{reg.p} \simeq \begin{cases} V_{tag}/V_{out.p} & (\text{if} \quad V_{out.p} > V_{tag}) \\ 1 & (\text{if} \quad V_{out.p} \leq V_{tag}). \end{cases}$

In (27), $\eta_{reg.p}$ denotes the efficiency of the output regulator. Although the SC-resistance of the proposed converter is larger than that of the conventional converter, the proposed converter can alleviate the loss in the output regulator, because the output voltage of the proposed converter is closer to the target voltage than that of the conventional converter. When the proposed converter satisfies the following condition:

$$\eta_{total.p} > \eta_{total.c}, \tag{28}$$

the proposed converter can realize higher power efficiency than the conventional converter. In (28), $\eta_{total.c}$ denotes the total efficiency of the conventional converter.

In the case of $V_{tag} = 2.2\,\mathrm{V}$, (28) is rewritten as

$$\eta_{reg.p} \times \frac{R_L}{R_L + 14R_{on}} \;>\; \eta_{reg.c} \times \frac{R_L}{R_L + (19/9)R_{on}}. \tag{29}$$

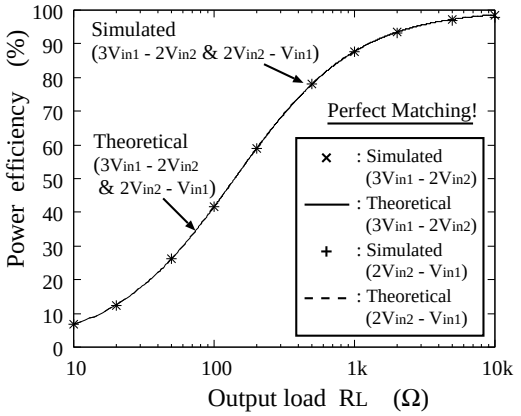

FIGURE 8. Simulated power efficiency as a function of output load R_L

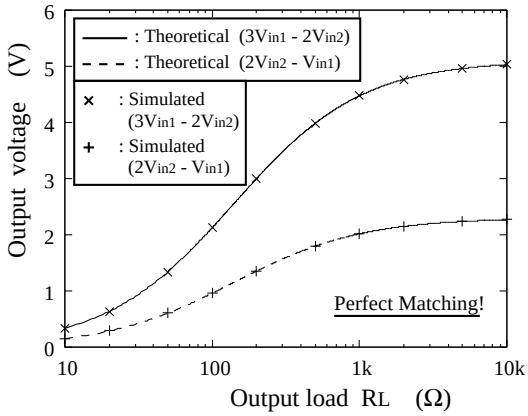

FIGURE 9. Simulated output voltage as a function of output load R_L

From (29), we have $R_L > 162R_{on}$

$$\text{if} \quad \eta_{reg.p} \simeq \frac{V_{tag}}{2V_{in2} - V_{in1}} = \frac{2.2}{2.3} \quad \text{and} \quad \eta_{reg.c} \simeq \frac{V_{tag}}{(2/3)V_{in1}} = \frac{3.3}{3.7}$$
$$\text{and} \quad D = 0.5 \quad \text{and} \quad V_{in1} = 3.7\,\text{V} \quad \text{and} \quad V_{in2} = 3\,\text{V}. \tag{30}$$

Concretely, in the case of $R_{on} = 1\Omega$, the total efficiency of the proposed converter is higher than that of the converter when R_L is larger than 162Ω.

On the other hand, in the case of $V_{tag} = 5\,\text{V}$, (28) is rewritten as

$$\eta_{reg.p} \times \frac{R_L}{R_L + 14R_{on}} > \eta_{reg.c} \times \frac{R_L}{R_L + (19/4)R_{on}}. \tag{31}$$

From (31), we have $R_L > 100R_{on}$

$$\text{if} \quad \eta_{reg.p} \simeq \frac{V_{tag}}{3V_{in1} - 2V_{in2}} = \frac{5}{5.1} \quad \text{and} \quad \eta_{reg.c} \simeq \frac{V_{tag}}{(3/2)V_{in1}} = \frac{5}{5.55}$$
$$\text{and} \quad D = 0.5 \quad \text{and} \quad V_{in1} = 3.7\,\text{V} \quad \text{and} \quad V_{in2} = 3\,\text{V}. \tag{32}$$

Concretely, in the case of $R_{on} = 1\Omega$, the total efficiency of the proposed converter is higher than that of the converter when R_L is larger than 100Ω.

4. **Simulation.** To confirm the validity of theoretical analysis, the properties of the proposed converter are investigated by SPICE simulations. To satisfy the conditions in the theoretical analysis, the simulation conditions were set to $V_{in1} = 3.7\,\text{V}$, $V_{in2} = 3\,\text{V}$ [3], $C_1 = C_2 = C_3 = 500\,\text{nF}$, $D = 0.5$, $R_{on} = 10\Omega$ [4] and $T = 1\mu\text{s}$.

Figure 8 shows the simulated power efficiency in the case of No.13 and No.18. Figure 9 shows the simulated output voltage in the case of No.13 and No.18. As Figures 8 and 9 show, the theoretical results correspond well with the simulated results. Consequently, the validity of the theoretical analysis described in Section 3 was confirmed. Of course, the power efficiency and the output voltage can be improved by using the power switch with low on-resistance.

[3]In the SPICE simulation, input source V_{in1} and V_{in2} were assumed as a lithium battery and a thermoelectric generator (TEG).

[4]The power switches were modeled by using SPICE macro-model.

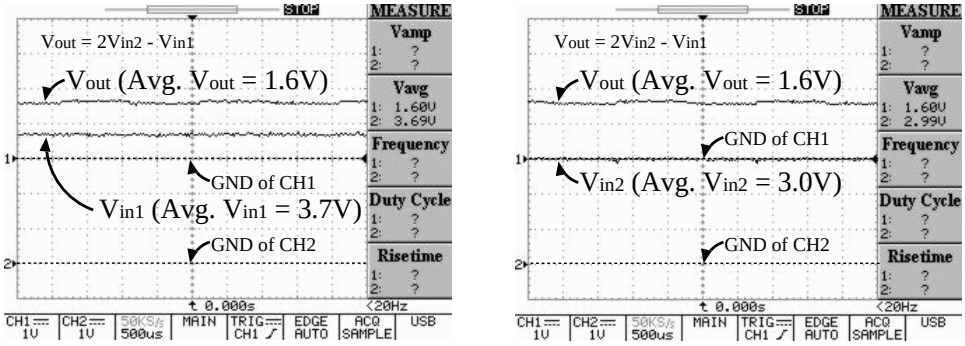

(a) (b)

FIGURE 10. Measured voltages in the case of No.13: (a) V_{out} vs. V_{in1} and (b) V_{out} vs. V_{in2}

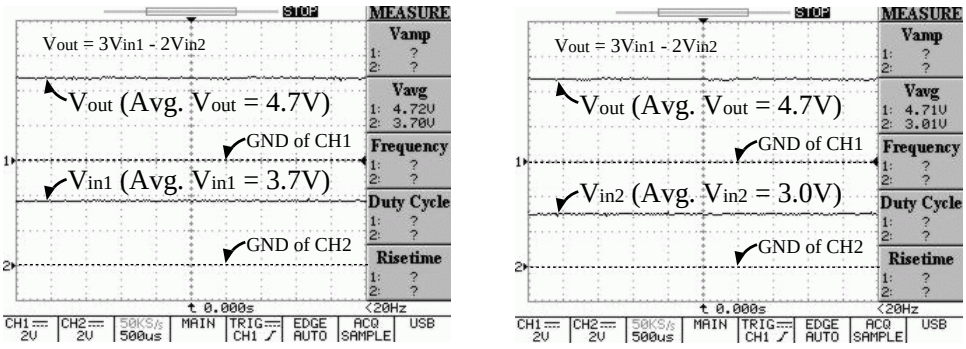

(a) (b)

FIGURE 11. Measured voltages in the case of No.18: (a) V_{out} vs. V_{in1} and (b) V_{out} vs. V_{in2}

5. **Experiment.** To confirm the validity of circuit design, experiments were performed regarding to the proposed converter shown in Figure 2(b). The experimental circuit was built with commercially available transistors 2SK2493 on a bread board, where $V_{in1} = 3.7\,\mathrm{V}$, $V_{in2} = 3\,\mathrm{V}$, $C_1 = C_2 = C_3 = 10\,\mu\mathrm{F}$, $R_L = 10k\Omega$ and $T = 2\mathrm{ms}$.

Figure 10 shows the measured output voltages in the case of No.13. Figure 11 shows the measured output voltages in the case of No.18. As Figures 10 and 11 show, unlike the conventional Dickson converter, the proposed converter can achieve step-up/step-down conversion [5].

6. **Conclusion.** A Dickson-type adder/subtractor DC-DC converter utilizing hybrid inputs has been proposed in this paper. To clarify properties of the proposed converter, circuit simulations, theoretical analyses and experiments were performed concerning a simple example of the proposed converter.

The SPICE simulations and experiments showed the following results: (1) The proposed converter provides more various kinds of output voltages than the three-stage ring-type DC-DC converter. The number of conversion ratios of the proposed converter is three times as large as that of the conventional converter. Therefore, the proposed converter

[5]In the experiment, the circuit properties such as power efficiency and ripple noise, were not examined, because the experimental circuit was built with commercially available transistors on the bread board. Only the circuit design was verified through the experiments, because the parasitic resistance of the bread board is very large unlike an IC chip.

can alleviate the energy loss caused by the output regulation. Furthermore, the proposed converter can realize smaller hardware cost than the conventional ring-type converter. The proposed converter can reduce more than 25% hardware cost than the conventional converter. (2) The proposed converter can provide not only the stepped-up voltage but also the stepped-down voltage, because the step-up/step-down conversion was confirmed by experiments. Although the conventional Dickson converter offers only the stepped-up voltage, the proposed converter can achieve step-up/step-down conversion by combining the battery energy and the clean energy. Therefore, the proposed converter will open up a new vista for mobile applications though the application target of the conventional Dickson converter is restricted due to a very limited conversion ratio. (3) The formulas obtained by the theoretical analysis are useful to estimate the characteristics the proposed converter, because the theoretical results corresponded well with the simulation results.

The IC implementation of the proposed equalizer is left to a future study.

REFERENCES

[1] S. Dalola, V. Ferrari, M. Guizzetti, D. Marioli, E. Sardini, M. Serpelloni and A. Taroni, Autonomous sensor system with power harvesting for telemetric temperature measurements of pipes, *IEEE Trans. Instrumentation and Measurement*, vol.58, no.5, pp.1471-1477, 2009.

[2] R. Y. Kim, J. S. Lai, B. York and A. Koran, Analysis and design of maximum power point tracking scheme for thermoelectric battery energy storage system, *IEEE Trans. Industrial Electronics*, vol.56, no.9, pp.3709-3716, 2009.

[3] S. Fan, K. Wang and L. Geng, Design and implementation of a mixed-signal boost converter with a novel multi-phase clock DPWM, *IEICE Electronics Express*, vol.7, no.14, pp.1091-1097, 2010.

[4] T. Yasufuku, K. Ishida, S. Miyamoto, H. Nakai, M. Takamiya, T. Sakurai and K. Takeuchi, Inductor and TSV design of 20-V boost converter for low power 3D solid state drive with NAND flash memories, *IEICE Electronics*, vol.E93-C, no.3, pp.317-323, 2010.

[5] T. Tanzawa and T. Tanaka, A dynamic analysis of the Dickson charge pump circuit, *IEEE J. Solid-State Circuits*, vol.32, no.8, pp.1237-1240, 1997.

[6] B. R. Gregoire, A compact switched-capacitor regulated charge pump power supply, *IEEE J. Solid-State Circuits*, vol.41, no.8, pp.1944-1953, 2006.

[7] J. H. Bong, Y. J. Kwon, D. Kim and K. S. Min, Negative charge pump circuit with large output current and high power efficiency, *IEICE Electronics Express*, vol.6, no.6, pp.304-309, 2009.

[8] S. J. Park, Y. G. Kang, J. Y. Kim, T. H. Han, Y. H. Jun, C. Lee and B. S. Kong, CMOS cross-coupled charge pump with improved latch-up immunity, *IEICE Electronics Express*, vol.6, no.11, pp.736-742, 2009.

[9] I. Y. Chung and J. Shin, New charge pump circuits for high output voltage and large current drivability, *IEICE Electronics Express*, vol.6, no.12, pp.800-805, 2009.

[10] P. H. Chen, K. Ishida, X. Zhang, Y. Okuma, Y. Ryu, M. Takamiya and T. Sakurai, 0.18-V input charge pump with forward body bias to startup boost converter for energy harvesting applications, *IEICE Electronics*, vol.94, no.4, pp.598-604, 2011.

[11] N. Hara, I. Oota, F. Ueno and T. Inoue, A ring type step-up switched capacitor DC-DC converter with low inrush current at start-up and low current ripplelin steady state, *IEICE Trans. C-II*, vol.J81-C-II, no.7, pp.600-612, 1998.

[12] N. Hara, I. Oota, F. Ueno, I. Harada and T. Inoue, Programable ring type switched capacitor DC-DC converters, *IEICE Trans. C-II*, vol.J82-C-II, no.2, pp.56-68, 1999.

[13] K. Eguchi, I. Oota, S. Terada and T. Inoue, A design method of switched-capacitor power converters by employing a ring-type power converter, *International Journal of Innovative Computing, Information and Control*, vol.5, no.10(A), pp.2927-2938, 2009.

[14] I. Doms, P. Merken, C. V. Hoof and R. P. Mertens, Capacitive power management circuit for micropower thermoelectric generators with a 1.4μA controller, *IEEE Solid-State Circuits*, vol.44, no.10, pp.2824-2833, 2009.

[15] K. Eguchi, I. Oota, S. Pongswatd, A. Julsereewong, K. Tirasesth and H. Sasaki, Synthesis and analysis of a dual-input parallel DC-DC converter designed by using switched capacitor techniques, *International Journal of Innovative Computing, Information and Control*, vol.7, no.4, pp.1675-1688, 2011.

[16] K. Eguchi, S. Pongswatd, K. Tirasesth, H. Sasaki, H. Zhu and T. Inoue, Design of a dual-input SC DC-DC converter realizing negative outputs, *IEEJ Trans. Electr. Electron. Eng.*, vol.6, no.5, pp.424-430, 2011.
[17] Y. H. Chang, Variable-conversion-ratio switched-capacitor-voltage-multiplier/divider DC-DC converter, *IEEE Trans. Circuit & Syst. – I*, vol.58, no.8, pp.1944-1957, 2011.
[18] Y. H. Chang, Design and analysis of multistage multiphase switched-capacitor boost DC-AC inverter, *IEEE Trans. Circuit & Syst.– I*, vol.58, no.1, pp.205-218, 2011.

Appendix. To compare the properties of the proposed converter with that of the conventional converter, the theoretical analysis concerning Figure 1(b) is performed in Appendix.

2/3× step-down conversion. In this section, the properties of the ring-type converter in the case of 2/3× step-down conversion are analyzed theoretically. The conditions of this theoretical analysis are the same as that of the theoretical analysis described in Section 3.

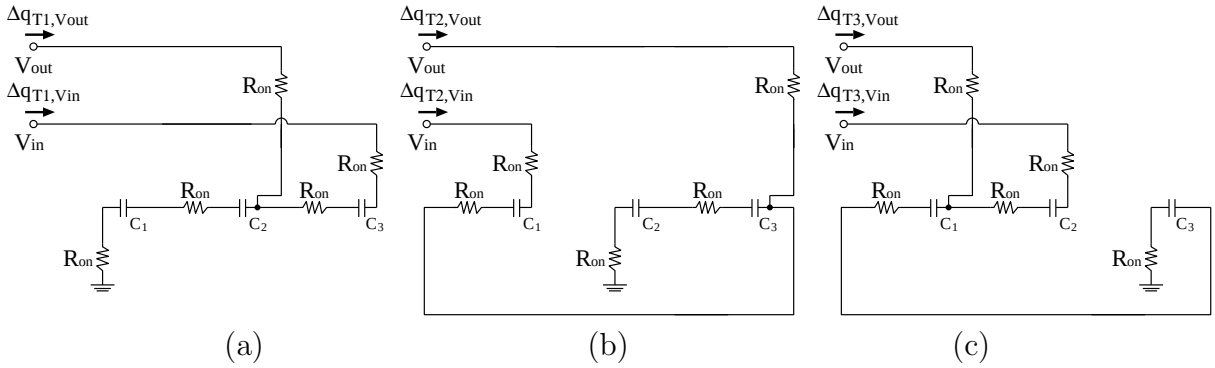

FIGURE 12. Instantaneous equivalent circuits of the ring-type converter in the case of 2/3× step-down conversion: (a) $State-T1$, (b) $State-T2$ and (c) $State-T3$

Figure 12 shows the instantaneous equivalent circuits in the case of 2/3× step-down conversion. In the steady state, the differential value of electric charges in C_k ($k = \{1,2,3,4\}$) satisfies

$$\Delta q_{T1}^k + \Delta q_{T2}^k + \Delta q_{T3}^k = 0, \quad \text{where} \quad T = T1 + T2 + T3 \quad (T1 = T2 = T3 = T_d). \tag{33}$$

In (33), Δq_{T1}^k, Δq_{T2}^k and Δq_{T3}^k denote electric charges in the case of $State-T1$, $State-T2$ and $State-T3$, respectively.

In the case of $State-T1$, $\Delta q_{T1,V_{in}}$ and $\Delta q_{T1,V_{out}}$ are given by

$$\Delta q_{T1,V_{in}} = \Delta q_{T1}^3 \quad \text{and} \quad \Delta q_{T1,V_{out}} = \Delta q_{T1}^2 - \Delta q_{T1}^3 = \Delta q_{T1}^1 - \Delta q_{T1}^3. \tag{34}$$

In the case of $State-T2$, $\Delta q_{T2,V_{in}}$ and $\Delta q_{T2,V_{out}}$ are given by

$$\Delta q_{T2,V_{in}} = \Delta q_{T2}^1 \quad \text{and} \quad \Delta q_{T2,V_{out}} = \Delta q_{T2}^3 - \Delta q_{T2}^1 = \Delta q_{T2}^2 - \Delta q_{T2}^1. \tag{35}$$

In the case of $State-T3$, $\Delta q_{T3,V_{in}}$ and $\Delta q_{T3,V_{out}}$ are given by

$$\Delta q_{T3,V_{in}} = \Delta q_{T3}^2 \quad \text{and} \quad \Delta q_{T3,V_{out}} = \Delta q_{T3}^1 - \Delta q_{T3}^2 = \Delta q_{T3}^3 - \Delta q_{T3}^2. \tag{36}$$

Using (34)-(36), the average current of the input and the output can be expressed by

$$\begin{aligned} & \overline{I_{in}} = (\Delta q_{T1,V_{in}} + \Delta q_{T2,V_{in}} + \Delta q_{T3,V_{in}})/T := \Delta q_{V_{in}}/T \\ \text{and} \quad & \overline{I_{out}} = (\Delta q_{T1,V_{out}} + \Delta q_{T2,V_{out}} + \Delta q_{T3,V_{out}})/T := \Delta q_{V_{out}}/T, \end{aligned} \tag{37}$$

where $\Delta q_{V_{in}}$ and $\Delta q_{V_{out}}$ are electric charges in terminal V_{in} and terminal V_{out}, respectively. Substituting (33)-(36) into (37), the relation between the input current and the output current is obtained as follows:

$$\overline{I_{in}} = -\frac{2}{3}\overline{I_{out}}. \tag{38}$$

In Figure 12, the energy consumed by resistors in one period, W_T, can be expressed by

$$W_T = W_{T1} + W_{T2} + W_{T3}, \tag{39}$$

where

$$W_{T1} = \frac{2R_{on}}{T_1}(\Delta q_{T1}^1)^2 + \frac{2R_{on}}{T_1}(\Delta q_{T1}^3)^2 + \frac{R_{on}}{T_1}(\Delta q_{T1}^1 - \Delta q_{T1}^3)^2$$
$$W_{T2} = \frac{2R_{on}}{T_2}(\Delta q_{T2}^1)^2 + \frac{2R_{on}}{T_2}(\Delta q_{T2}^2)^2 + \frac{R_{on}}{T_2}(\Delta q_{T2}^2 - \Delta q_{T2}^1)^2$$
$$\text{and} \qquad W_{T3} = \frac{2R_{on}}{T_3}(\Delta q_{T3}^2)^2 + \frac{2R_{on}}{T_3}(\Delta q_{T3}^3)^2 + \frac{R_{on}}{T_3}(\Delta q_{T3}^3 - \Delta q_{T3}^2)^2.$$

From (33)-(36) and (37), consumed energy (39) can be rewritten as

$$W_T = \frac{19R_{on}}{9T}(\Delta q_{V_{out}})^2. \tag{40}$$

Thus, from (11) and (40), we have the SC resistance R_{SC} as follows:

$$R_{SC} = \frac{19}{9} \cdot R_{on}. \tag{41}$$

Using (38) and (41), the equivalent circuit in the case of $2/3\times$ step-down conversion can be expressed by the following determinant:

$$\begin{bmatrix} \overline{V_{in}} \\ \overline{I_{in}} \end{bmatrix} = \begin{bmatrix} 3/2 & 0 \\ 0 & 2/3 \end{bmatrix} \begin{bmatrix} 1 & R_{SC} \\ 0 & 1 \end{bmatrix} \begin{bmatrix} \overline{V_{out}} \\ -\overline{I_{out}} \end{bmatrix}. \tag{42}$$

Therefore, the power efficiency in the case of $2/3\times$ step-down conversion can be expressed by (14).

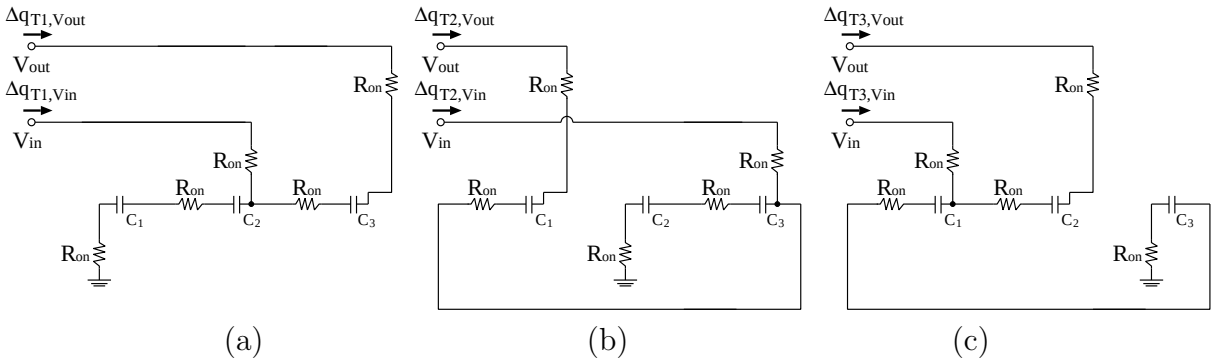

FIGURE 13. Instantaneous equivalent circuits of the ring-type converter in the case of $3/2\times$ step-up conversion: (a) $State - T1$, (b) $State - T2$ and (c) $State - T3$

3/2× step-up conversion. Figure 13 shows the instantaneous equivalent circuits in the case of 3/2× step-up conversion. In the case of $State - T1$, $\Delta q_{T1,V_{in}}$ and $\Delta q_{T1,V_{out}}$ are given by

$$\Delta q_{T1,V_{in}} = \Delta q^2_{T1} - \Delta q^3_{T1} = \Delta q^1_{T1} - \Delta q^3_{T1} \quad \text{and} \quad \Delta q_{T1,V_{out}} = \Delta q^3_{T1}. \tag{43}$$

In the case of $State - T2$, $\Delta q_{T2,V_{in}}$ and $\Delta q_{T2,V_{out}}$ are given by

$$\Delta q_{T2,V_{in}} = \Delta q^3_{T2} - \Delta q^1_{T2} = \Delta q^2_{T2} - \Delta q^1_{T2} \quad \text{and} \quad \Delta q_{T2,V_{out}} = \Delta q^1_{T2}. \tag{44}$$

In the case of $State - T3$, $\Delta q_{T3,V_{in}}$ and $\Delta q_{T3,V_{out}}$ are given by

$$\Delta q_{T3,V_{in}} = \Delta q^1_{T3} - \Delta q^2_{T3} = \Delta q^3_{T3} - \Delta q^2_{T3} \quad \text{and} \quad \Delta q_{T3,V_{out}} = \Delta q^2_{T3}. \tag{45}$$

Substituting (33), (43), (44) and (45) into (37), the relation between the input current and the output current is obtained as follows:

$$\overline{I_{in}} = -\frac{3}{2}\overline{I_{out}}. \tag{46}$$

In Figure 13, the energy consumed by resistors in one period, W_T, can be expressed by

$$W_T = W_{T1} + W_{T2} + W_{T3}, \tag{47}$$

where

$$W_{T1} = \frac{2R_{on}}{T_1}(\Delta q^1_{T1})^2 + \frac{2R_{on}}{T_1}(\Delta q^3_{T1})^2 + \frac{R_{on}}{T_1}(\Delta q^1_{T1} - \Delta q^3_{T1})^2$$

$$W_{T2} = \frac{2R_{on}}{T_2}(\Delta q^1_{T2})^2 + \frac{2R_{on}}{T_2}(\Delta q^2_{T2})^2 + \frac{R_{on}}{T_2}(\Delta q^2_{T2} - \Delta q^1_{T2})^2$$

and $$W_{T3} = \frac{2R_{on}}{T_3}(\Delta q^2_{T3})^2 + \frac{2R_{on}}{T_3}(\Delta q^3_{T3})^2 + \frac{R_{on}}{T_3}(\Delta q^3_{T3} - \Delta q^2_{T3})^2.$$

From (33), (37), (43), (44) and (45), consumed energy (47) can be rewritten as

$$W_T = \frac{19R_{on}}{4T}(\Delta q_{V_{out}})^2. \tag{48}$$

Thus, from (11) and (48), we have the SC resistance R_{SC} as follows:

$$R_{SC} = \frac{19}{4} \cdot R_{on}. \tag{49}$$

Using (46) and (49), the equivalent circuit in the case of 3/2× step-up conversion can be expressed by the following determinant:

$$\begin{bmatrix} \overline{V_{in}} \\ \overline{I_{in}} \end{bmatrix} = \begin{bmatrix} 2/3 & 0 \\ 0 & 3/2 \end{bmatrix} \begin{bmatrix} 1 & R_{SC} \\ 0 & 1 \end{bmatrix} \begin{bmatrix} \overline{V_{out}} \\ -\overline{I_{out}} \end{bmatrix}. \tag{50}$$

Therefore, the power efficiency in the case of 3/2× step-up conversion can be expressed by (16).